Table II. Optical Spectral Data and ESR Parameters

	$[L_1M]^{2+}$	$(L_1\text{-}2H)M$	$[(L_1\text{-}4H)M]^{2-}$	$[L_2M]^{2+}$	$(L_2\text{-}2H)M$	$(L_3\text{-}2H)M$
			M = Ni			
λ_{max},[a] nm	820, 736, 570[a]	440[a]	432[c]	820, 736, 564[a]	590[d]	596[d]
			M = Cu			
λ_{max}, nm	626[a]	524[a]		630[a]	550[d]	550[d]
g_{iso}[b]	2.127[a]	2.101[a]		2.126[a]	2.099[d]	
A_{iso},[b] G	74	75		75	92	
A_N,[b] G	12.5	14.1		12.0	12.5	
no. of N-shf lines	5	9		5	5	

[a] Solution in CH_3OH/H_2O (1/1). [b] Isotropic spectra related to solutions studied at 295 K. [c] Solution H_2O. [d] Solution in CH_2Cl_2.

nitrogen atoms adjacent to the copper ion through the observation of the superhyperfine (N-shf) lines.[6]

All the isotropic spectra (solutions studied at room temperature) considered in the present work (Table II) show the well-known hyperfine structure of four lines due to coupling of the electron with the nuclear spin ($I = {}^3/_2$) of the copper ion. In addition, interaction of the electron with the adjacent ^{14}N nuclei ($I = 1$) results in a superhyperfine structure clearly discernible on the high-field component of the hyperfine spectrum. In all complexes but one, five N-shf lines are observed with a separation of ca. 12.5 G, indicating that the environment of the copper ion is N_2O_2. In one case, namely $(L_1\text{-}2H)Cu$, the number of N-shf lines increases to nine in accordance with four nitrogen atoms surrounding the copper ion.

Electronic Spectroscopy. Considering the positions of the absorption maximum (λ_{max}) reported in Table II, it appears that similar trends are observed for the copper and nickel complexes. However, the spread of the observed λ_{max} values is markedly smaller in the former series than in the second one.

Among the three neutral copper complexes, the same value (550 mm) is observed for $(L_2\text{-}2H)Cu$ and $(L_3\text{-}2H)Cu$ whereas $(L_1\text{-}2H)Cu$ displays a lower value (524 nm). This is in accordance with the change in the coordination sphere established by ESR data (from N_2O_2 in the former complexes to N_4 in the latter one) and the generally accepted assumption that a shift of the absorption maximum toward shorter wavelengths is associated with an increase in the number of the nitrogen atoms adjacent to the metal center.[7] The high values of ca. 630 nm characterizing the cationic complexes likely reflect a tetragonal deformation.[8]

Regarding the nickel complexes, identical spectra, characteristic of an octahedral geometry, are obtained for the cationic complexes. This contrasts with the behavior of the related neutral complexes, which display very different values of the absorption maximum. In addition, we must note that similar values of λ_{max} are observed for $(L_1\text{-}2H)Ni$ and $[(L_1\text{-}4H)Ni]^{2-}$ on the one hand and $(L_2\text{-}2H)Ni$ and $(L_3\text{-}2H)Ni$ on the other hand. Recalling that in this last complex the environment of the nickel can be nothing but N_2O_2 and that deprotonation of the amide groups likely favors a N_4 environment in $[(L_1\text{-}4H)Ni]^{2-}$, we think that, as is the case for the related copper complexes, the shift of λ_{max} from 590 nm in $(L_2\text{-}2H)Ni$ to 440 nm in $(L_1\text{-}2H)Ni$ reflects a change of the coordination mode from N_2O_2 to N_4.

Conclusion

The ESR and visible spectroscopic data herein obtained for $[L_1Cu]^{2+}$ and $(L_1\text{-}2H)Cu$ are almost identical with those previously reported by Lim and McCool[4] for the isolated cationic complex and the nonisolated neutral species, respectively. However, comparative scrutiny of the chemical behavior and spectroscopic data relating to the whole set of copper and nickel complexes prepared from L_1, L_2, and L_3 affords converging arguments to demonstrate that, in all cases, (i) not only the ligand L_3 but also L_1 and L_2 are in the enamine form and (ii) the first step of the deprotonation process concerns the protons of the enamine functions and not those of the amide groups.

Therefore, the presence of four nitrogen atoms adjacent to the metal ion in the $(L_1\text{-}2H)M$ complexes (M = Cu, Ni) implies that the nitrogen atoms of the intact primary amide groups are able to coordinate the metal ion at least in solution.

---

(6) Wiersma, A. K.; Windle, U. J. *J. Chem. Phys.* **1964**, *68*, 2316.

(7) Bjerrum, J.; Balhausen, C. J.; Jørgensen, C. K. *Acta Chem. Scand.* **1954**, *8*, 1275.

(8) Hathaway, B. J. *Struct. Bonding (Berlin)* **1984**, *57*, 55.

Contribution from the Department of Chemistry,
Texas A&M University, College Station, Texas 77843

Pillaring of Layered Zirconium and Titanium Phosphates

A. Clearfield* and B. D. Roberts

Received February 22, 1988

In the preceding two decades, a new class of two-dimensional porous materials has been synthesized from smectite clay minerals.[1] This was accomplished by swelling the clays and inserting large species between the layers to keep them apart. Smectite clays are able to swell in water because of their low layer charge and, thus, easily intercalate organic guest molecules or large inorganic polymers.[2] In general, the organically pillared structures suffer from the thermal instability of the organic component, which limits their use in catalysis. Since a major motive for the preparation of these materials is to provide new catalytically active large-pore structures, robust pillars are required. Therefore, attention was focused on the use of the aluminum Keggin ion, $[Al_{13}O_4(OH)_{24}\cdot 12H_2O]^{7+}$, or the zirconium tetramer, $[Zr(OH)_2\cdot 4H_2O]_4{}^{8+}$, as pillars.[3-5] Ideally, the inserted inorganic species will be arranged so as to leave large spaces, of the order of 10–12 Å, between them. They have therefore been viewed as pillars propping open the layers so as to provide porosity for sorption or enhanced catalytic activity. From its early beginnings, a considerable literature has developed, details of which are given in recent reviews.[2,6,7] However, there are a large number of clays and nonsilicious layered compounds that do not swell in water and therefore are not accessible to pillaring by conventional methods. We were interested in pillaring such compounds, and in developing several methods applicable to large classes of layered materials so as to produce potential sorbents and catalysts with a range of acidic and shape-selective properties. In this note we describe a method of accomplishing this goal with zirconium and titanium phosphates. It entails first intercalating an amine between the layers and then exchanging the cationic pillar for the interlamellar alkylammonium ion. We had earlier shown that large charged complexes could be incorporated between the layers in this manner.[8]

Experimental Section

α-Zirconium (α-ZrP) and α-titanium phosphates (α-TiP), $M(HPO_4)_2\cdot H_2O$, and γ-zirconium (γ-ZrP) and γ-titanium phosphates (γ-TiP), $M(HPO_4)_2\cdot 2H_2O$, were prepared in the usual way.[9,10] Butylamine

---

* To whom correspondence should be addressed.

Table I. X-ray Diffraction Powder Patterns of α-Zirconium Phosphate and the α-ZrP/n-Butylamine Intercalate

α-ZrP			α-ZrP/n-butylamine		
d, Å	I/I_0	index (hkl)	d, Å	I/I_0	index
7.56	75	002	18.6	100	(002)
4.48	40	110	9.33	10	(004)
4.45	25	$20\bar{2}$	6.20	3.5	(006)
3.57	100	112	4.61	4.5	(008)
3.52	55	$60\bar{4}$	4.54	4.0	
3.29	5		4.08	3.5	
3.21	5		4.0	3.5	
3.08	5		3.64	2.5	
3.02	2		2.65	7.0	
2.63	30				
2.61	35				

was intercalated into 1 g of the layered compounds as 0.1 M aqueous solution by using 100 mL of solution /g of solid phosphate. After the mixture was stirred for 2 h, the solid was recovered by filtration and washed twice with 10-mL portions of distilled water. The solid was then reslurried in 35 mL of water, and 16 mL of a 15% solution of the basic aluminum chloride hydroxide (Reheis, Microdry) was added. The mixture was stirred and heated at 70 °C for 90 min and then cooled to room temperature and filtered; the product was washed and air-dried. Several variants as to concentration of the aluminum solution, ratio of reactants, and temperatures were tried.

Analysis for aluminum was carried out by neutron activation at the Texas A&M Nuclear Science Center or by treating the solid with 20 mL of boiling HCl and analyzing the diluted solution by ICP. The residue was then collected, calcined at 1000 °C, and weighed as the pyrophosphate. X-ray powder patterns were obtained with Cu Kα radiation on a Seifert-Scintag PAD-II automated powder diffractometer. IR spectra were taken with a Perkin-Elmer 580B spectrophotometer, though the IR spectra were generally uninformative due to H-bond broadening of the hydroxyl-region bands. The thermogravimetric, surface area (LN$_2$, BET), and plug-molecule sorption measurements were carried out with a Cahn RG microbalance and associated vacuum system. Surface areas were measured at liquid-nitrogen temperature, while the remaining sorption work was done at room temperature. The saturation pressure of each plug molecule was determined in the vacuum system just before sorption was done and P/P_0 values of 0.80 or less were used. Mercury porosimetry measurements were made with a Micromeritics PoreSizer 9310 porosimeter.

Results and Discussion

Butylamine readily intercalates into the layered group IV phosphates to the extent of 2 mol/formula weight of phosphate.[11] In the process, the interlayer spacing increases from 7.6 to 18.6 Å in the α-zirconium and α-titanium phosphates. This increase in interlayer spacing then allows the exchange of polymeric aluminum species for alkylammonium ions to take place. Typical X-ray powder patterns for the aluminum-pillared titanium and zirconium phosphates are shown in Figure 1. These patterns should be compared with the data in Table I, which gives the major X-ray reflections for α-ZrP and its butylamine intercalate. The first reflection in the X-ray pattern represents the interlayer spacing or d_{002} in the unpillared crystal.[12,13] It is seen in Figure 1 that several different values of the interlayer spacing were obtained and that the peaks are broad and are of low intensity, indicative of a high degree of disorder. This behavior is also common with pillared clays.[6] The aluminum Keggin ion may be considered to be a prolate spheriod with dimensions of ~9.5 × 7 Å. Since the layer in α-zirconium phosphate is 6.6 Å thick we might expect the final pillared products to have interlayer spacings of 13.6–16.1 Å depending upon how the ion is situated in the interlamellar space. It is seen that samples Al no. 216 and Al no. 219 fall within this range, but sample Al no. 217 has a much larger spacing.[14] The reflections for α-ZrP and the butylamine intercalate are sharp compared to those sown in Figure 1. Thus, whenever some of the butylamine is not exchanged, the pattern for the intercalate is clearly evident in the X-ray powder pattern. Carbon analysis for samples 216, 217, and 219 were all well below 1% (no. 216, 0.4%; no. 217, 0.7%; no. 219, 0.15%). If the pH is allowed to go below 3, some exchange of protons for amine may occur prior to pillaring and then the X-ray pattern of α-ZrP is also observed. The patterns shown in Figure 1 contain no evidence that proton exchange rather than aluminum pillaring has occurred. We shall return to this point after considering other features of the pillared products.

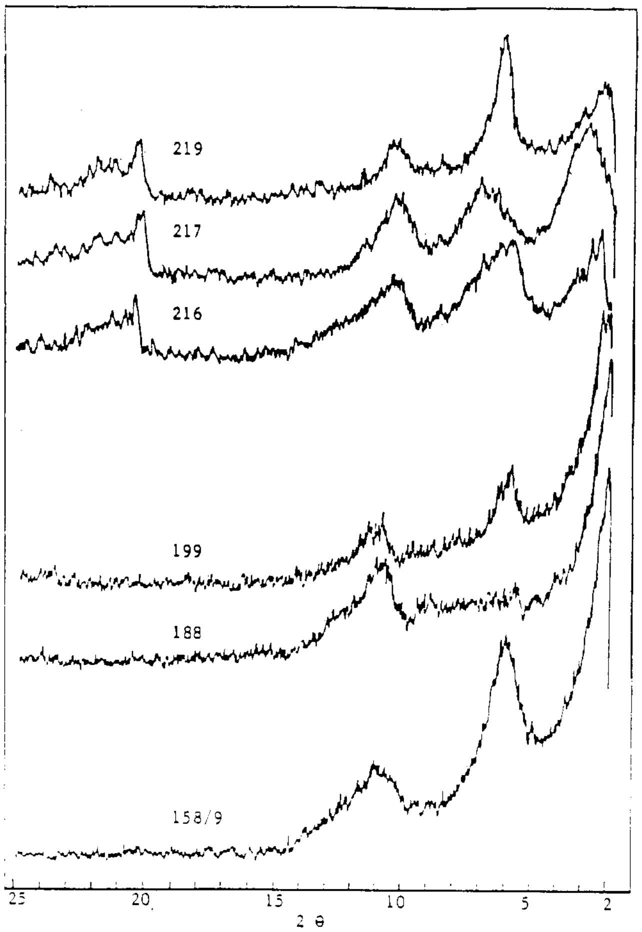

Figure 1. X-ray diffraction patterns of aluminum [(Al$_{13}$O$_4$(OH)$_{24}$·12H$_2$O)$^{7+}$] pillared zirconium and titanium phosphates: Zirconium phosphates: α-ZrP(12:336), no. 217; α-ZrP(12:15), no. 216; α-ZrP(9:48), no. 219. Titanium phosphates: γ-TiP, no. 158/9; α-TiP(12:17), no. 188; α-TiP(2.5:48), no. 199. The numbers in parentheses indicate the concentration of H$_3$PO$_4$ and the time of reflux in hours, respectively, required to prepare the α-ZrP or α-TiP from a gel.

---

(1) Barrer, R. M. *Hydrothermal Chemistry of Zeolites*; Academic: New York, 1982.
(2) Pinnavaia, T. J. *Science (Washington, D.C.)* **1983**, *220*, 365.
(3) Lahav, N.; Shani, V.; Shabtai, J. *Clays Clay Miner.* **1978**, *26*, 107.
(4) Brindley, G. W.; Semples, R. E. *Clays Clay Miner.* **1977**, *26*, 229.
(5) Yamanaka, S.; Brindley, G. W. *Clays Clay Miner.* **1978**, *26*, 21.
(6) Pinnavaia, T. J. In *Heterogeneous Catalysis*; Shapiro, B., Ed.; Texas A&M University Press: College Station, TX, 1985; p 145.
(7) Clearfield, A. In *Surface Organo-Metallic Chemistry: Molecular Approaches to Surface Catalysis*; Proceedings of NATO Workshop, May 25–30, 1986, Le Rouret, France; Reidel: Dordrecht, The Netherlands, 1987.
(8) Clearfield, A.; Tindwa, R. M. *Inorg. Nucl. Chem. Lett.* **1979**, *15*, 251.
(9) Clearfield, A.; Duax, W. L.; Medina, A. S.; Smith, G. D.; Thomas, J. R. *J. Phys. Chem.* **1969**, *73*, 3424.
(10) Clearfield, A.; Blessing, R. H.; Stynes, J. A. *J. Inorg. Nucl. Chem.* **1968**, *30*, 2249.
(11) Clearfield, A.; Tindwa, R. M. *J. Inorg. Nucl. Chem.* **1978**, *41*, 871.
(12) Clearfield, A.; Smith, G. D. *Inorg. Chem.* **1969**, *8*, 431.
(13) Clearfield, A.; Nancollas, G. H.; Blessing, R. H. *Ion Exchange and Solvent Extraction*; Marinsky, J. A., Marcus, Y., Eds.; Dekker: New York, 1973.
(14) Disordered structures always exhibit large scattering effects at low 2θ values as seen in Figure 1. Thus, other low-angle peaks may exist below 2° 2θ but are less likely. The one shown in sample no. 217 is however unambiguous.

Table II. Surface Area and Sorption Data for Pillared Titanium and Zirconium Phosphates

			sorption (samples degassed at 200 °C)							
			PFTBA		cyclohexane		*n*-pentane		H_2O	
sample	sample starting material	surface area[a]	% wt	P/P_0[b]	% wt	P/P_0	% wt	P/P_0	% wt	P/P_0
Al no. 158/9	γ-TiP(cryst)	121			1.41	0.207			9.0	0.07
					4.47	0.60			22.6	0.83
Al no. 188	α-TiP(12:17)	169			5.2	0.14	1.77	0.14		
			34.0	0.74	13.0	0.58	3.70	0.57		
Al no. 199	α-TiP(2.5:48)	183	20.0	0.10						
			36.5	0.79						
Al no. 216	α-ZrP(12:15)	30	9.0	0.75						
Al no. 217	α-ZrP(12:336)	35								
Al no. 219	α-ZrP(9:48)	37								
TiP gel		59	6.4	0.04[c]						
			9.0	0.11						
α-TiP(2.5:48)		11								

[a] N_2 BET (m^2/g); degassed at 200 °C. [b] P_0: 100 Torr for cyclohexane, 140 Torr for *n*-pentane, ~0.5 Torr for PFTBA. [c] Uptake is by intercalation.

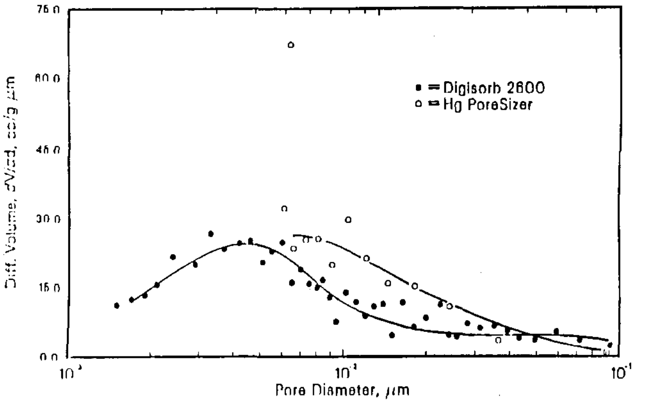

Figure 2. Pore size distribution for pillared α-TiP, sample no. 235C, as determined by mercury porosimetry (open circles) and N_2 sorption (filled circles).

A 20-g batch of Al_{13} pillared α-TiP (no. 235C) was prepared to the same specifications[15] as a smaller initial sample of Al no. 199. Analysis of an air-dried portion gave 9.1% Ti, 14.2% Al, and 36.1% PO_4. Thermogravimetric analysis showed that constant weight was achieved at about 350 °C with the loss of 34% water. On the assumption that the Keggin ion is exchanged unchanged, the formula can be represented as $Ti(HPO_4)_{0.48}(PO_4)_{1.52}[Al_{13}O_4(OH)_{24}(H_2O)_{12}]_{0.216}\cdot 3.5H_2O$. This formula requires 9.1% Ti, 14.4% Al, 35.5% PO_4, and 30.7% H_2O.[16] The pillared sample gave a surface area of 237 m^2/g after dehydration under vacuum at 200 °C. The comparable value obtained by mercury porosimetry was 137 m^2/g, showing that pores smaller than 60-Å diameter were responsible for 100 m^2/g of the total surface area. The actual pore size distribution is shown in Figure 2, where it is seen that an appreciable fraction of pores are in the 10–30-Å diameter range. Heating a sample of the pillared α-TiP in air to 350 °C for 4 h reduced the surface area to 182 m^2/g, showing that the pore structure was largely maintained. Unpillared α-TiP condenses to an amorphous TiP_2O_7 of low surface area at this temperature.[17]

Analysis of more than a dozen pillared samples of α-zirconium phosphate showed that they contained variable aluminum contents ranging from 7.4% to 13.8% on a dry basis. Furthermore, the interlayer spacings varied from 13.0 to 16.1 Å and there was no correlation between aluminum content and interlayer *d* spacing. However, when the zirconium phosphate was highly crystalline, there was a greater tendency to form the products with 24–30-Å interlayer spacings.

The term highly crystalline needs further explanation. We have shown that the degree of crsytallinity of α-zirconium phosphate is strongly dependent upon the concentration of H_3PO_4 in which the gel is refluxed and upon the reflux time.[13,18,19] Refluxing in 12 M H_3PO_4 for 14 days results in crystallites of 1–2-μm average size. These crystallites tended to yield pillared products with the larger (27–30 Å) interlayer spacings. The less crystalline zirconium phosphate (refluxed in 12 M H_3PO_4 for 15 h) yielded products of the Al no. 216 and Al no. 219 type. Surface areas of all pillared zirconium phosphates were in the range 30–35 m^2/g as compared to 1–8 m^2/g for the unpillared phosphates. Furthermore, the pillared products did not intercalate amines or ammonia, nor did they sorb molecules such as 2-propanol into the interlamellar space. Thus, we may conclude that the zirconium phosphate products are nonporous species in which the pillars have "stuffed" the interlamellar regions, i.e. filled the available space.

In contrast, both α- and γ-titanium phosphates yielded pillared products with high surface areas, and these products sorbed relatively large molecules, as shown in Table II. The pillared products were degassed at 200 °C for 12 h prior to exposure to the sorbate. Large amounts of perfluorotributylamine (PFTBA), which has a kinetic diameter of 10 Å, were sorbed at low vapor pressures. The porous pillared titanium phosphates retained more than 70% of their surface area after heating to 400 °C. Unpillared titanium phosphates condense to amorphous pyrophosphates at this temperatures.[17]

^{27}Al NMR spectra of microdry solutions were similar to those reported by Pinnavaia[6] and indicated that the solutions contained appreciable amounts of $Al(H_2O)_6^{3+}$ and polymerized species other than the aluminum Keggin ion. Thus, we believe that, while the Keggin ion is one of the pillaring species, other species may also be incorporated. Therefore, a combination of Keggin ion pillars and smaller species could be responsible for the stuffed character of the pillared zirconium phosphates. In preliminary experiments it was found that exchange of $Al(H_2O)_6^{3+}$ with the butylamine intercalates of α-zirconium phosphate gave a product with a 9.4-Å interlayer spacing in agreement with the previously obtained Al^{3+}-exchanged phase.[20] We then prepared a solution that contained only the Al_{13} Keggin ion according to ^{27}Al NMR spectra. This was done by electrolytically dissolving aluminum metal in an $AlCl_3$ solution. The end product of the pillaring reaction obtained from this solution also had a 9.4-Å (9.4° 2θ) interlayer spacing, indicating a breakdown of Keggin ion to simple

---

(15) Ten grams of α-TiP was slurried in 500 mL of 0.2 M butylamine for 4 h, filtered off, washed with two 50-mL portions of distilled water, and then reslurried in 200 mL of distilled water. To this slurry was added 160 mL of a 15% microdry solution, and the mixture was heated at 60–70 °C for 90 min. The recovered solid was washed with three 20-mL portions of distilled water and air-dried.

(16) This amount of water includes the 0.24 mol from condensation of the monohydrogen phosphate group.

(17) Clearfield, A.; Frianeza, T. *J. Catal.* **1984**, *85*, 398.

(18) Clearfield, A.; Oskarsson, Å.; Oskarsson, C. *Ion Exch. Membr.* **1972**, *1*, 91.

(19) Clearfield, A.; Oskarsson, Å., Kullberg, L. *J. Phys. Chem.* **1974**, *78*, 1150.

(20) Quayle, L. Ph.D. Thesis, Texas A&M University, College Station, TX, 1981.

Al^{3+} ions. Thus, the idea that the stuffed condition may result from the pores, formed by the pillars, being filled by smaller species is plausible but not the only possible explanation. Why this occurs with Zr and not with titanium is an intriguing question. Electron micrographs show that the α-ZrP and α-TiP platelet retain their shape upon pillaring, but the titanium platelets exhibit a corrugated appearance about the edges, which may indicate large pores allowing access to the interior of the solid. Further investigations are in progress as is also an extension of the technique described here to other classes of layered compounds.

Acknowledgment. Funding for this work was provided by a grant from Amoco Chemical Co. and Texaco Incorporated, U.S.A. We gratefully acknowledge their support. We also wish to thank L. J. Czarnecki for determining the mercury porosimeter data.

Contribution from the Department of Chemistry,
Bloomsburg University, Bloomsburg, Pennsylvania 17815

Comparative Study of the Electronic Structures of *N*,*N'*-Diethyldithiocarbamate and Pyrrole-*N*-carbodithioate and Their Nickel(II) Complexes

Wayne P. Anderson* and Donald M. Baird†

Received October 16, 1987

Dithiocarbamates, which can be represented by resonance forms A–C, have been used extensively as ligands in inorganic, bioinorganic, and analytical chemistry.[1] These ligands fall into two broad classes. Dialkyldithiocarbamates, such as *N*,*N'*-diethyldithiocarbamate (Et_2dtc^-), are most often employed. Recent interest, however, has focused on dithiocarbamates derived from aromatic amines such as pyrrole.[2] Because of the aromatic character of pyrrole, resonance form C is assumed to be less important in pyrrole-*N*-carbodithioate ($pdtc^-$) than it is in the dialkyl analogues.[2] This shift in electron density results in a less positive nitrogen atom and less negative sulfur atoms in pyrrole-*N*-carbodithioate. The coordination behavior of the ligand is thereby altered. It has also been proposed that pyrrole-*N*-carbodithioate forms stronger π-bonds with the metal than the dialkyl analogues.[3]

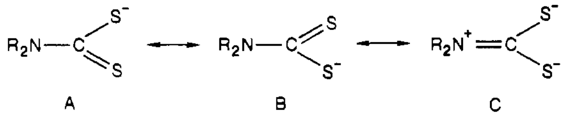

Since an increasing number of workers are using aromatic dithiocarbamate ligands to control the physical and chemical properties of dithiocarbamate complexes,[3-9] it seemed important to determine whether quantum-mechanical models agree with qualitative ideas about the relative importance of resonance forms A–C and the importance of metal–ligand π-bonding in pyrrole-*N*-carbodithioate complexes. We also wished to determine whether any insight could be gained concerning the relative reactivities of coordinated dithiocarbamate ligands from such quantum-mechanical models. Previous CNDO/2 calculations have been performed on the dimethyldithiocarbamate complex of nickel(II),[10,11] but no MO calculations have been reported on the analogous pyrrole-*N*-carbodithioate system. Results of INDO/S[12,13] calculations on the free diethyldithiocarbamate and pyrrole-*N*-carbodithioate ligands and their nickel(II) complexes are reported in this note, and the effects of including sulfur d orbitals are assessed. Details of the theoretical model are summarized in the Appendix.

Table I. Wiberg Bond Indices[a,b]

	Et_2dtc^-	$pdtc^-$
	No Point Charge	
C–S	1.21 (0.24)	1.30 (0.33)
	[1.27 (0.29)]	[1.37 (0.38)]
C–N	1.33 (0.36)	1.13 (0.18)
	[1.28 (0.33)]	[1.09 (0.16)]
	+1 Point Charge[c]	
C–S	1.13 (0.16)	1.21 (0.23)
	[1.18 (0.17)]	[1.27 (0.27)]
C–N	1.53 (0.55)	1.29 (0.32)
	[1.48 (0.53)]	[1.25 (0.31)]
	Ni(II) Complex	
C–S	1.13 (0.16)	1.20 (0.23)
	[1.17 (0.19)]	[1.25 (0.27)]
C–N	1.48 (0.51)	1.25 (0.29)
	[1.45 (0.51)]	[1.23 (0.29)]
Ni–S	0.71 (0.02)	0.70 (0.02)
	[0.81 (0.06)]	[0.79 (0.06)]

[a] Numbers in parentheses are Wiberg π-bond indices between orbitals perpendicular to the NiS_4 plane. [b] Numbers in brackets refer to results when d orbitals are included on sulfur. [c] Assuming +1 charge at the site where the metal would be located.

Results and Discussion

Wiberg bond indices[14] for *N*,*N'*-diethyldithiocarbamate, pyrrole-*N*-carbodithioate, and their corresponding nickel(II) complexes are listed in Table I. Since the Wiberg bond index has approximately the same value as the traditional bond order (i.e., a single bond has a Wiberg index of 1.0, and a double bond 2.0), it is easily related to classical resonance forms. In agreement with previous arguments, the C–S index is higher and the C–N index lower in $pdtc^-$ and $Ni(pdtc)_2$ than in Et_2dtc^- and $Ni(Et_2dtc)_2$.[15] Bonding to the metal has a comparable effect on the two ligands. The C–S index is lowered and the C–N index raised, implying that resonance form C contributes more to the bonding in the complex than in the free ligand. Experimentally, this leads to an increase in the C–N stretching frequency upon coordination to the metal.[16] The effect of coordination to nickel(II) on the Wiberg indices of the two ligands can be mimicked by the presence of a +1 point charge at the site where the metal is located. This suggests that much of the change in electron distribution upon coordination is a result of the electrostatic influence of the metal. The magnitudes of the Wiberg indices are changed slightly by including d orbitals on sulfur, but the trends are identical.

---

* To whom correspondence should be addressed.

† Current address: Department of Chemistry, Florida Atlantic University, Boca Raton, FL 33431.

(1) (a) Coucouvanis, D. *Prog. Inorg. Chem.* **1970**, *11*, 233. (b) Coucouvanis, D. *Prog. Inorg. Chem.* **1979**, *26*, 301. (c) Burns, R. P.; McCullough, F. P.; McAuliffe, C. A. *Adv. Inorg. Chem. Radiochem.* **1980**, *23*, 211.

(2) Bereman, R. D.; Nalewajek, D. *Inorg. Chem.* **1977**, *16*, 2687.

(3) El A'mma, A. G.; Drago, R. S. *Inorg. Chem.* **1977**, *16*, 2975.

(4) Bereman, R. D.; Churchill, M. R.; Nalewajek, D. *Inorg. Chem.* **1979**, *18*, 3112.

(5) Bereman, R. D.; Nalewajek, D. J. *J. Inorg. Nucl. Chem.* **1978**, *40*, 1313.

(6) Bereman, R. D.; Baird, D. M.; Vance, C. T.; Hutchinson, J.; Zubieta, J. *Inorg. Chem.* **1983**, *22*, 2316.

(7) Herrick, R. S.; Templeton, J. L. *Inorg. Chem.* **1986**, *25*, 1270.

(8) Baird, D. M.; Fanwick, P. E.; Barwick, T. *Inorg. Chem.* **1985**, *24*, 3753.

(9) Baird, D. M.; Bereman, R. D.; Moreland, C. G. *Polyhedron* **1983**, *2*, 59.

(10) Pilipenko, A. T.; Savranskii, L. T.; Zubenko, A. I. *Koord. Khim.* **1981**, *7*, 1613.

(11) Pilipenko, A. T.; Savransky, L. I.; Zubenko, A. I. *THEOCHEM*, **1981**, *86*, 29.

(12) Zerner, M. C.; Loew, G. H.; Kirchner, R. F.; Mueller-Westerhoff, U. T. *J. Am. Chem. Soc.* **1980**, *102*, 589.

(13) Herman, Z. S.; Kirchner, R. F.; Loew, G. H.; Mueller-Westerhoff, U. T.; Nazzal, A.; Zerner, M. C. *Inorg. Chem.* **1982**, *21*, 46.

(14) Wiberg, K. B. *Tetrahedron* **1968**, *24*, 1083.

(15) The Wiberg indices are sensitive to the bond lengths used in the calculation. If the C–S and C–N bond lengths in $pdtc^-$ are set equal to those in Et_2dtc^- (C–S = 1.706 Å, C–N = 1.326 Å), the C–S index is lowered by 0.05 to 1.32 and the C–N index is raised by 0.05 to 1.14 in calculations that include sulfur d orbitals. The trends remain the same, however.

(16) van Gaal, H. L. M.; Diesveld, J. W.; Pijpers, F. W.; van der Linden, J. G. M. *Inorg. Chem.* **1979**, *18*, 3251.

0020-1669/88/1327-3240$01.50/0